INTERNATIONAL JOURNAL OF RESEARCH
In Advanced Engineering Technologies

Volume 6, Issue 1 JAN 2017

Design and Implementation of Fuzzy Logic Based Voltage Control of A 3- Phase Power Converter

R L S Naveen Kumar [1]
nven.ravirala@gmail.com[1]

C. Srinivasulu [2]
eeedepttkrec@gmail.com[2]

[1]PG Scholar, Dept of EEE, Teegala Krishna Reddy Engineering College Affiliated to JNTUH, Meerpet, Saroor Nagar, Ranga Reddy, Telangana, India.
[2] Guide and HOD, Associate Professor, Dept of EEE, Teegala Krishna Reddy Engineering College Affiliated to JNTUH, Meerpet,Saroor Nagar, Ranga Reddy, Telangana, India.

***Abstract*— This project presents the operation of a distributed generation (DG) system driven by a dc-dc step-up converter and a dc-ac voltage source inverter (VSI) interfaced with the power grid by Fuzzy Controller. To create a stable mode when different kinds of loads are connected locally or when working under contingency, the step-up converter must regulate the dc link voltage, allowing the VSI to stabilize its terminal voltage. The power flow between the grid and the DG is controlled by applying a power/voltage method that regulates the amplitude and the displacement of the grid voltage synthesized by the DG, while a phase-locked loop algorithm is used to synchronize the grid and DG by fuzzy. Additionally, a set of simulations are performed independent of the load type or its work regime (whether it is connected to the grid). The effectiveness of the proposed method is evaluated by experimental results by using Fuzzy Logic Controller.**

***Index Terms*—Distributed generation (DG), islanding modes, power converters.**

I. INTRODUCTION

The use of distributed generation (DG) sources is currently being considered as a solution to the growing problems of energy demand [1]. Apart from the consequent reduction in the size of the generating plants and the possibility of modular implementation, DG systems based on renewable energy sources [2] (photovoltaic, fuel cells, and storage systems such as ultra capacitors and batteries [1]) are of great interest due to their low environmental impact [3] and technical advantages such as improvements in voltage levels and reduced power losses when a DG system is installed in radial lines [4]. DG systems also promote cogeneration [5] and improve overall system efficiency [6].

A DG system operating at high performance requires a detailed evaluation of the feeder where the DG will be installed [7], plus an assessment of the load type the DG must supply locally and its working regime. Without these requirements, the effects of DG may be more harmful than beneficial: the insertion of new generation sources in the distribution system may cause transient effects due to switching operations, changing short-circuit levels, lower margin of stability, and inversion of the power flow through the distribution system, causing erroneous operations of the protection devices and islanding in part of the system [8].

In addition, the DG operation should not exceed the limits established by international standards for the following parameters: harmonic distortion [9], voltage imbalance, voltage fluctuations, and fast transients, whether the local load is unbalanced, nonlinear, or a dynamic load, such as a motor [10]. Recently, the use of power or current in the d-q synchronous reference frame [11]–[14] as control variables to command the voltage source inverter (VSI) connected to the grid has generated considerable interest from the scientific community.

With either method, before or after the contingency takes place, the control variable remains the same, making the DG operate with limited capability to supply the load. On the other hand, two control algorithms were proposed to improve the grid-connected and intentional-islanding operations methods in [15], in which the DG system must detect the situation and switch from power or current to voltage as a control variable to provide constant rms voltage to the local loads. In [16] and [17], the power flow is determined by controlling the amplitude and angle of displacement between the voltage produced by the DG and the grid voltage [18], i.e., the control variable is the same before and after the islanding mode occurs.

The voltage control provides the capability to supply different kinds of loads to the DG system, such as linear, nonlinear, motor, balanced, or unbalanced [19], even if the DG operates in the islanding mode. These kinds of controls are suitable for DGs operating in parallel as each of the DGs are connected to the grid through a distribution transformer (DT) [20]. Conversely, the other approaches introduced in [21], [22] are more effective. This paper analyzes the effects caused by 50 to 5000-kVA DG sources inserted into the distribution system, whether the local load is linear or nonlinear, or if the grid is operating under abnormal conditions. Section II details the method used to drive both converters. Section III discusses the technique to control the power flow through the grid. Sections IV and V show the simulations and experimental setup to confirm the previous analysis, while the main points presented in this paper appear in the conclusion.

II. CHARACTERISTICS OF THE DG SYSTEM

Fig. 1 shows a diagram of the system used to analyze a typical connection of a DG system to a specific feeder, although

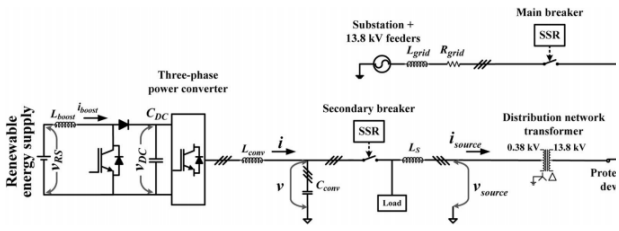

Fig. 1. General diagram of the distributed generation system.

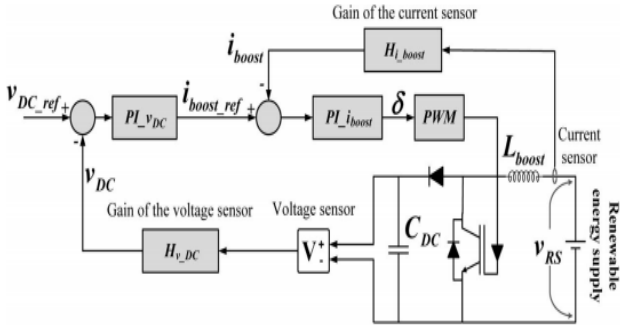

Fig. 2. Block diagram of the dc voltage/current control.

studies to determine the best site for DG insertion should be performed before the operation analysis [7]. A power plant represents a secondary source (DG systems), while in this study the standard grid is a basic configuration system found in 1547 standard (simulated system) [23] or a California Instruments LX 4500 source (experimental setup). Furthermore, the primary energy used in the proposed DG system is the same as the previously mentioned renewable energy sources. A dc-dc converter is employed to equalize the dc link voltage and deliver energy for fast transients when required by the local load, while a dc-ac converter is used to guarantee the power quality delivered to customers (local load) and the specific feeder. To avoid disturbances between the dc-ac converter and the feeder, a phase-locked loop (PLL) algorithm [11] associated with the zero voltage crossing detectors was used [24], [25]. Appendix I shows the design procedure for key passive components.

A. DC-DC Converter

A dc-dc step-up converter was used as an interface between the dc source and dc link of the three-phase dc-ac converter, as shown in Fig. 2. The step-up converter boosts the dc voltage and supplies the fast transients of energy required for the local load, thereby minimizing disturbances in the feeder current. The behavior of the step-up converter is similar to a voltage source, and the power it delivers to the grid depends on the point of maximum power (PMP) defined by the dc source [1]. The PMP is obtained using a tracking algorithm [26], based on the primary

energy source. To keep the converters operating in a stable mode, proportional-integral (PI) controllers were used as a control.

TABLE I

PI CURRENT PARAMETERS OF THE DC-DC CONVERTER

F_{CL} (Hz)	mf (°)	V_{DC} (V)	L_{boost} (mH)	H_{i_boost}
400	80	1,000	5	1/250

TABLE II

PI VOLTAGE PARAMETERS OF THE DC-DC CONVERTER

F_{CL} (Hz)	mf (°)	V_{DC} (V)	C_{DC} (mF)	H_{v_DC}
50	60	1,000	12	1/1,500

technique to stabilize the Lboost current and dc voltage (V_{dc}). A method based on phase-margin (mf) and cutoff frequency (F_{cl}) was used to obtain the PIs constants (1) and (2) [2], [16], where the open loop gain (G_{ol}), angular frequency (ω_{fcl}), and mf define the PIs constants (k_{prop} and k_{int}) [16]

$$k_{prop}\frac{G_{OL}}{\omega_{F_{CL}}} = 1 \quad (1)$$

$$k_{int} = k_{prop}\frac{\omega_{F_{CL}}}{tan(mf)}. \quad (2)$$

Tables I and II display the main design parameters to determine the PIs constants of the boost converter [2], namely, H_i_boost and H_v_DC gains for the dc current and voltage sensors, respectively.

B. DC-AC Converter

Closed-loop controls of the output current and voltage were implemented to guarantee inverter voltage quality. PIs controllers were also used as the control technique, while the design method of

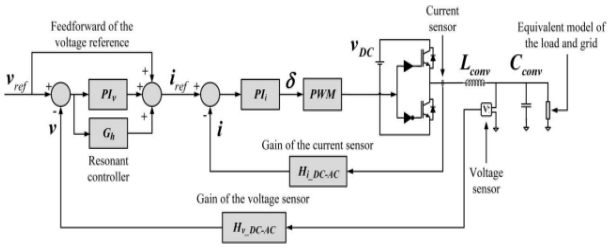

Fig. 3. Block diagram of the ac voltage/current control.

TABLE III

CURRENT PI PARAMETERS OF THE DC-AC CONVERTER

F_{CL} (Hz)	mf (°)	V_{DC} (V)	L_{conv} (mH)	$H_{i\_DC\text{-}AC}$
1,200	70	1,000	2	1/250

TABLE IV

VOLTAGE PI PARAMETERS OF THE DC-AC CONVERTER

F_{CL} (Hz)	mf (°)	V_{DC} (V)	C_{conv} (μF)	$H_{v\_DC\text{-}AC}$
120	70	1,000	15	1/360

these PIs is the same as that used in the dc-dc step-up converter [16]. Since the closed-loop cutoff frequency of the PI current controller was chosen one decade below the switching frequency, the PI of the current retains a good compensation capability in the frequency range of interest.

To improve this capability, a feed forward of the reference voltage could be used to compensate the residual error in the closed-loop gain at low frequencies [27], [28]. Due to its high power and the need for a reduced switching frequency, the voltage controller exhibits a low regulation bandwidth (a few hundred Hertz).

To improve the control response of the output voltage regulator for fundamental and harmonic components, a resonant controller (3)[29] is placed in parallel along with the conventional voltage PI, thereby reducing the converter impedance [16], [30]. In (3),(h) is the harmonic order, (ωch) is the bandpass around the resonance angular frequency, (ω0) is the resonance angular frequency, and (kih) is the resonant controller gain [2], [11], [16]–[28].

A general block diagram demonstrating the control v is shown in Fig. 3. Tables III and IV present the main design parameters of the ac PIs, wherein Hi_DC−AC and Hv_DC−AC are the ac current and voltage sensors gains, respectively

$$G_h = k_{ih}\frac{2\omega_{ch}s}{s^2 + 2\omega_{ch}s + (h\omega_0)^2}. \quad (3)$$

C. Grid Characteristics

In the simulations, the complete distribution system found in 1547 standard [23] is composed of 13.8-kV feeders connected to a 69-kV radial line through 69/13.8-kV substation transformers, as shown in Fig. 1. To insert the DG at the

TABLE V

MODIFIED PARAMETERS OF THE CONVERTERS

V_{DC} (V)	C_{DC} (μF)	H_{i_boost}	H_{v_DC}	$H_{i\_DC\text{-}AC}$
330	2,800	1/12	1/360	1/12

distribution system, a 13.8/0.38 kV distribution network transformer is required to equalize the voltage levels. The line model employed in the simulations took into account the Bergeron's traveling wave method used by the Electromagnetic Transients Program, which utilized wave propagation phenomena and line end reflections.

Additionally, a set of switches was inserted between the DGs and distribution system, isolating them from each other to avoid the DG system supplies loads (loads placed in neighboring feeders where the DG was installed) connected to the high voltage side of the distribution transform. Due to the high level of power and voltage, 12 kHz was used as the PWM switching frequency for both converters. An experimental setup was built to substantiate the DG operation. The grid was represented by a California Instruments LX 4500 source and an isolated 220/220-V transformer; the power converter was commanded by an Analog Devices 21992 DSP, while the parameters to design the controllers are those in Tables I–IV, except for the parameters in Table V, which were calculated for a 3-kVA low scale prototype.

To maintain their similarity with the simulations, the switching and sampling frequencies were also kept at 12 kHz. The grid parameters (4) and (5) used in the experimental setup were calculated to have the same dynamic response as the simulated system [31], [32]. The main grid parameters of the equivalent model used in the experimental setup are represented by *Lgrid*, *Rgrid*, *PSC*, *f*, and *VA2source* (inductance and resistance (losses), short-circuit power, rated frequency, and rms voltage (phases A and B), respectively)

$$L_{grid} = \frac{V_{AB_{source}}^2}{2\pi P_{SC} f} \quad (4)$$

$$R_{grid} = \frac{(2\pi f)L_{grid}}{X}, \quad 1 < X < 100. \quad (5)$$

D. Synchronization Algorithm

To connect the DG to the grid, it is essential to synchronize both systems, which is done by means of a PLL algorithm that computes the average of the internal product between V_{source} and the synchronous voltage ($v\perp$) [24], [33]. If this equals zero

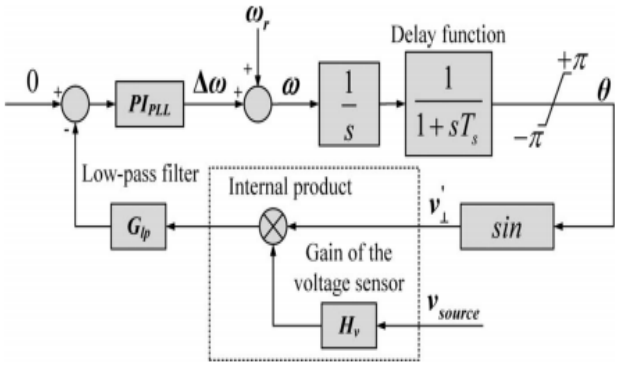

Fig. 4. PLL algorithm.

in steady-state regime, $v\perp$ and V_{source} are perpendicular and synchronized [25]. The integration of the angular frequency (ω) then defines the θ angle (θ = wt) used as the argument to produce $v\perp$. Due to the high sampling

and switching frequency Ts ≈ 0, the delay block can be dismissed in the PLL closed loop transfer function

$$H_{CL} = \frac{PI_{PLL}}{s} = \frac{k_p s + k_i}{s^2 + k_p s + k_i}. \quad (6)$$

To compare the characteristic equation of the prototype transfer function with the PLL closed-loop transfer function (7), PI constants (8) and (9) can be adjusted by choosing the most suitable values for the natural undamped frequency (ωn) and damping ratio (ξ). To avoid stability problems, ωn should ideally be greater than one or two periods of the fundamental frequency, and the maximum overshoot lower than 30%. A general description of the PLL algorithm is found in Fig. 4, where ωr, Δω, and Hv are the rated angular frequency (= 2π60), adjusted angular frequency, and voltage sensor gain (1/360) (voltage measured at the grid), respectively

$$\underbrace{s^2 + k_p s + k_i}_{\text{Characteristic equation of the PLL transfer function}} = \underbrace{s^2 + 2\xi\omega_n s + \omega_n^2}_{\text{Characteristic equation of the Prototype transfer function}} \quad (7)$$

$$k_p = 2\xi\omega_n \quad (8)$$

$$k_i = \omega_n^2. \quad (9)$$

III. POWER CONTROL THROUGH THE FEEDER

Energy produced by the renewable energy sources can be transferred to the grid by controlling the amplitude of the voltage produced by the DG, and the angle between the grid voltage and the DG voltage (β angle) through a coupling inductor (LS) [16], [18]. This serves as an additional inductance placed to connect the DG to the grid, or the leakage inductance of the DT. If LS is a DT parameter, V_{source} must be measured on the high voltage side of the distribution network transformer. To achieve a controlled power flow from the DG to the grid, the DG voltage angle (V A) must be ahead of the grid voltage angle (Vsource). When this occurs, the DG delivers active power to the grid, as shown in Fig. 5 [28].

The same analysis can be applied to the ac voltage amplitude produced by the DG: if the amplitude of V A is greater than Vsource the DG delivers reactive power to the grid; however, if the amplitude of V A is less than V A source the DG absorbs reactive power from the grid.

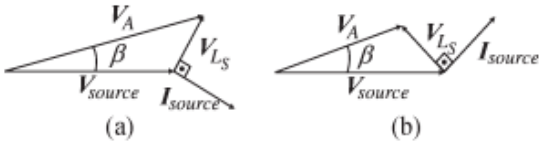

Fig. 5. Phasor diagrams. (a) Delivering active and reactive power. (b) Delivering active and absorbing reactive power.

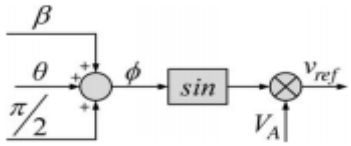

Fig. 6. Determination of the voltage reference.

The β angle is determined by the average power flowing to the grid (Psource), the connection reactance (XLS), the rms phase voltage (VAsource) synthesized by the grid, and the rms voltage produced (VA) by the DG according to (10). After defining the β angle, the DG voltage amplitude of V A must be adjusted according to (11), where VAsource and XLS are the same parameters described in (10). If Qsource = 0 the unity power factor (PF) to the feeder is obtained [34]. Additionally, LS is designed for a small voltage variation on the ac local voltage produced by the dc-ac inverter [16]. In Fig. 6, the voltage reference (vref) of the dc-ac power converter is determined by displacing θ by π/2 and adding the β angle to the result. The φ angle is then used as the argument of a sinusoidal function and multiplied by VA to obtain the voltage reference that must be synthesized at the VSI terminals

$$\beta = sin^{-1}\left(\frac{P_{source}\,|X_{LS}|}{V_{A_{source}} V_A}\right) \quad (10)$$

$$V_A = \sqrt{2}\left(\frac{V_{A_{source}}^2 - Q_{source}\,|X_{LS}|}{V_{A_{source}}\cos\beta}\right). \quad (11)$$

A. FUZZY LOGIC CONTROLLER

In FLC, basic control action is determined by a set of linguistic rules. These rules are determined by

the system. Since the numerical variables are converted into linguistic variables, mathematical modeling of the system is not required in FC. The FLC comprises of three parts: fuzzification, interference engine and defuzzification. The FC is characterized as; i. seven fuzzy sets for each input and output. ii. Triangular membership functions for simplicity. iii. Fuzzification using continuous universe of discourse. iv. Implication using Mamdani"s „min" operator. v. Defuzzification using the „height" method.

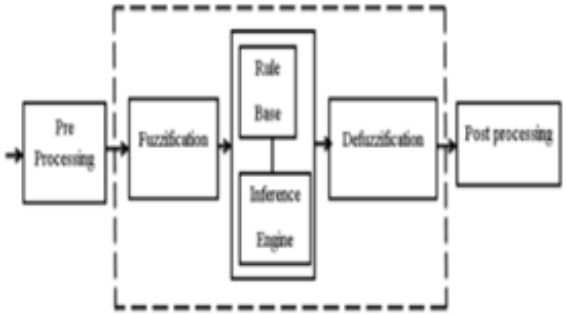

Fuzzy Logic Controller

Fuzzification:

Membership function values are assigned to the linguistic variables, using seven fuzzy subsets: NB (Negative Big), NM (Negative Medium), NS (Negative Small), ZE (Zero), PS (Positive Small), PM 5 (Positive Medium), and PB (Positive Big). The partition of fuzzy subsets and the shape of membership *CE(k) E(k)* function adapt the shape up to appropriate system. The value of input error and change in error are normalized by an input scaling factor

Change In Error	Error						
	NB	**N M**	**NS**	**Z**	**PS**	**PM**	**PB**
NB	PB	PB	PB	PM	PM	PS	Z
NM	PB	PB	PM	PM	PS	Z	Z
NS	PB	PM	PS	PS	Z	NM	NB
Z	PB	PM	PS	Z	NS	NM	NB
PS	PM	PS	Z	NS	NM	NB	NB
PM	PS	Z	NS	NM	NM	NB	NB
PB	Z	NS	NM	NM	NB	NB	NB

Table1. Fuzzy Rules

In this system the input scaling factor has been designed such that input values are between -1 and +1. The triangular shape of the membership function of this arrangement presumes that for any particular *E(k)* input there is only one dominant fuzzy subset. The input error for the FLC is given as

$$E(k) = \frac{P_{ph(k)} - P_{ph(k-1)}}{V_{ph(k)} - V_{ph(k-1)}}$$

$$CE(k) = E(k) - E(k-1)$$

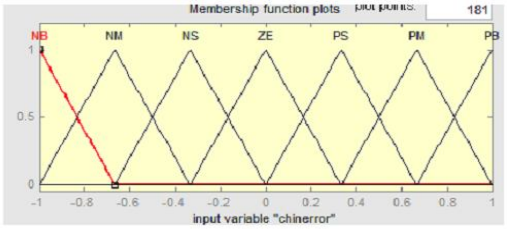

Membership Functions

Interference Method:

Several composition methods such as Max–Min and Max-Dot have been proposed in the literature. In this paper Min method is used. The output membership function of each rule is given by the minimum operator and maximum operator. Table 1 shows rule base of the FLC.

Defuzzification:

As a plant usually requires a non-fuzzy value of control, a defuzzification stage is needed. To compute the output of the FLC, „height" method is used and the FLC output modifies the control output. In recent years, the number and variety of applications of fuzzy logic have increased significantly. The applications range from consumer products such as cameras, camcorders, washing machines, and microwave ovens to industrial process control, medical instrumentation, decision-support systems, and portfolio selection. To understand why use of fuzzy logic has grown, you must first understand what is meant by fuzzy logic. Fuzzy logic has two different meanings. In a narrow sense, fuzzy logic is a logical system, which is an extension of multivalve logic. However, in a wider sense fuzzy logic (FL) is almost synonymous with the theory of fuzzy sets, a theory which relates to classes of objects with unsharp boundaries in which membership is a matter of degree.

In this perspective, fuzzy logic in its narrow sense is a branch of fl. Even in its more narrow definition, fuzzy logic differs both in concept and substance from traditional multivalve logical systems.

In fuzzy Logic Toolbox software, fuzzy logic should be interpreted as FL, that is, fuzzy logic in its wide sense. The basic ideas underlying FL are explained very clearly and insightfully in Foundations of Fuzzy Logic. What might be added is that the basic concept underlying FL is that of a linguistic variable, that is, a variable whose values are words rather than numbers.

In effect, much of FL may be viewed as a methodology for computing with words rather than numbers. Although words are inherently less precise than numbers, their use is closer to human intuition. Furthermore, computing with words exploits the tolerance for imprecision and thereby lowers the cost of solution.

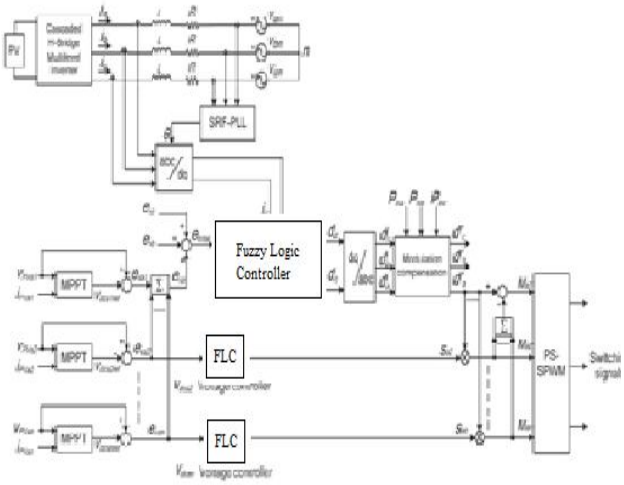

Fig. 6. Control scheme for three-phase modular cascaded H-bridge multilevel PV inverter by Using Fuzzy Logic Controller.

IV. SIMULATION ANALYSIS

Simulations were performed using MatLab/Simulink software.

A. Connection and Power Transfer:

Two procedures are required to connect the DG system to the feeder. First, an algorithm must be used to synchronize Vsource with the voltage produced by the converter v. After synchronization, the algorithm to detect zero crossing of vsource must be initiated. When this is done, the switch connecting both systems is closed, minimizing the transient effects to the feeder (which occur up to 0.2 s).

Subsequently, a soft transfer (40 kVA/s) of power starts at 0.25 s of the simulation range, followed by a base load operation. Due to the method used—synchronization and soft transfer of power—minimal disturbances are observed in the grid, as shown in Figs. 7 and 8. However, when the soft transfer of power is completed, two groups of resistive loads are connected within a short time interval (one, demanding 70 kW, is inserted at 0.8 s; the other, demanding 60 kW, is connected at 1.3 s).

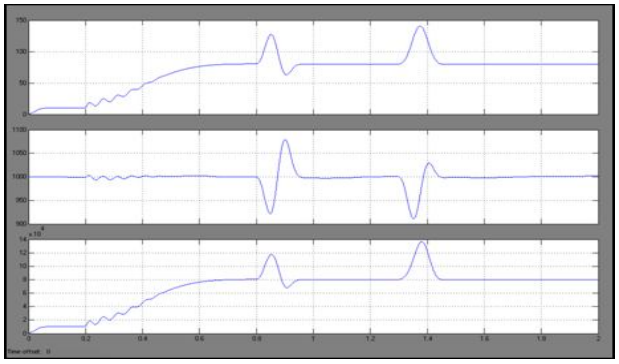

Fig. 7. Operation of the boost converter.

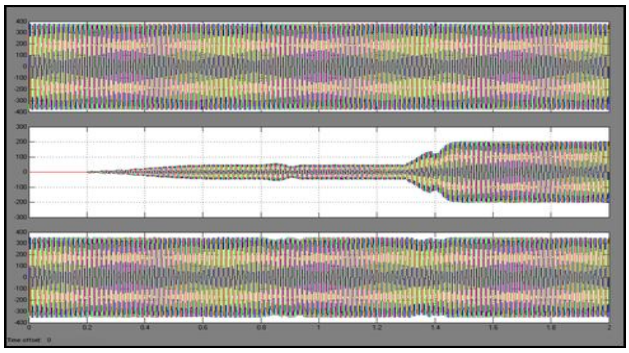

Fig. 8. DG absorbing active power from the grid.

Due to load capability, the current flowing through the grid inverts its direction, making additional power come from the grid. At the moment of the load connection, most of the electric variables are submitted to fast transients.

However, this is not observed in the grid voltages because the short-circuit power of the grid is higher than the short-circuit power of the DG. To verify the power quality delivered to customers, total harmonic distortion (THD) of the DG voltage is well below 5%, whereas the PF is close to unity.

B. Nonlinear Load:

Another issue to be analyzed is the influence of a nonlinear load connected to the DG terminals. In this case, the control technique used to synthesize the ac voltage by the inverter plays an important role.

In fact, it reduces the impedance of the inverter, making the DG system compensate the local load harmonics. In this test, the load is inserted at 0.4 s and the DG is connected to the grid at 2 s, remaining so for 6 s. To observe the system's capability, the minimal value of active and reactive power flows through the grid, with the nonlinear load represented by a non controlled three-phase power.

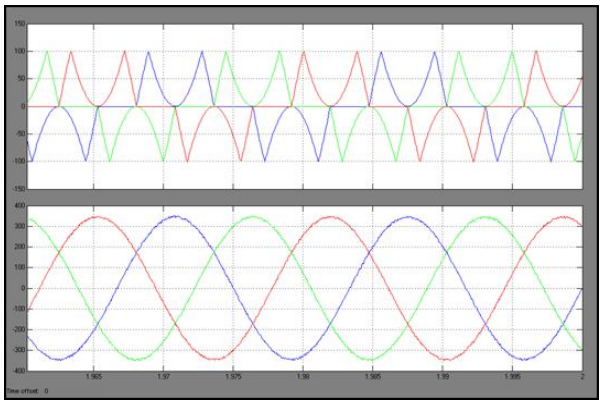

Fig. 9. Zoom of the load currents and voltages produced by the DG with nonlinear load.

rectifier plus RC load that demands around 50 kVA from the DG. In this operation mode, the THD of the voltage imposed by the VSI rises to 3%, even with the resonant controller compensating the 1st, 3rd, and 5th to 15th harmonics, however, the THD of the load current achieves more than 115%.

To observe what happens with the DG system, a short time interval (1.96 to 2.04 s) before and after the connection with the grid is presented in Fig. 9, which demonstrates the DG capability to supply nonlinear loads in the connected or isolated modes.

C. Islanding Mode Consideration:

When a short-circuit occurs on the high voltage side of the DT, the protection devices closest to the event disconnect the grid from the distribution system in order to avoid stability problems [35], [36]. However, the DG remains connected, forming a local area whose mode of operation may be dangerous if the local load demand is greater than the power produced by the DG.

To avoid this, the DG must identify the contingency as soon as possible and disconnect it from the local area. To understand the effects on the grid and power converters, the following series of events was performed. First, a balanced three-phase linear load demanding almost 25 kW was connected to the DG terminals at the beginning of the simulation.

At 1.8 s, the power produced by the DG system was reduced (pDC drops from 125 kW to 100 kW), and a 75-kW three phase linear load was connected to the DG terminals to obtain a minimal power level exchanged with the grid, which, as reported in literature [11], is the most difficult situation to identify the islanding mode. Fig. 10 identifies the effect of the islanding mode compared with the load connection or power transfer to the grid. In each case, the islanding mode did not affect the dc link voltage and power, or the ac power flow through the grid, which was not the case for the load connection or power transfer.

D. Islanding and Reconnection to the Feeder:

Another important aspect of the DG operation is the islanding mode followed by a reconnection. As above, the test:

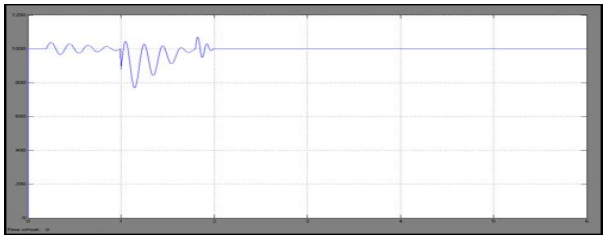

10(a)

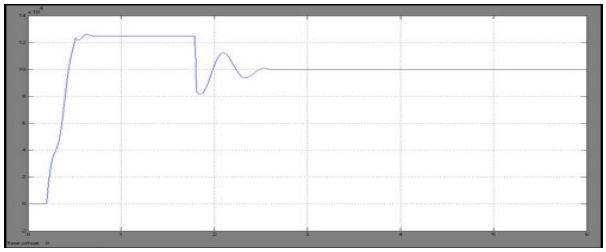

10(b)

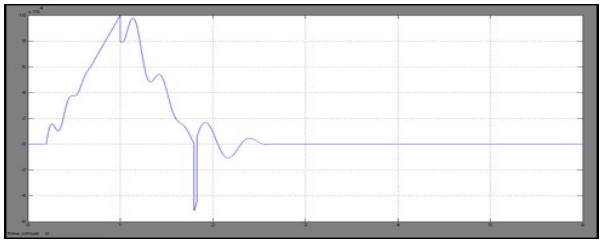

10(c)

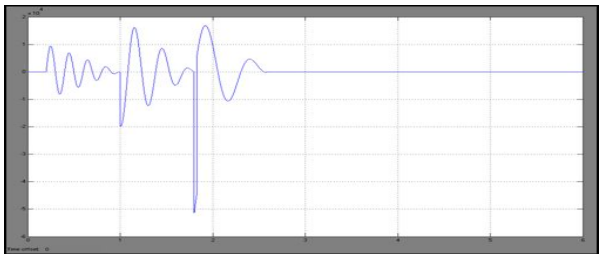

10(d)

Fig. 10. Islanding with zero power flow.

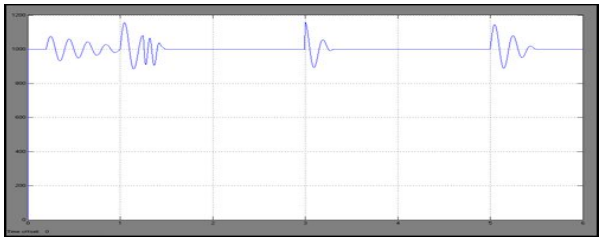

11(a)

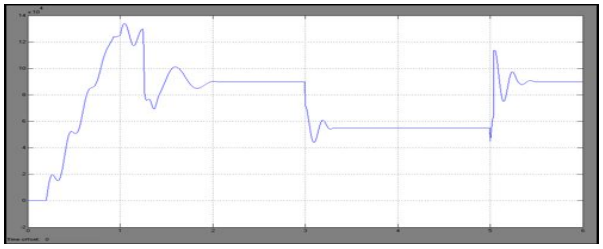

11(b)

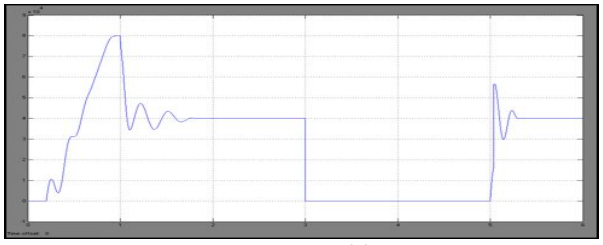

11(c)

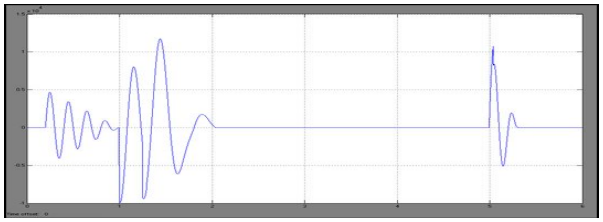

11(d)

Fig. 11. Islanding and reconnection with nonzero power flow

performed here considers a limited power level exchanged with the grid.

At the beginning of the simulations, a balanced three-phase linear load demanding 30 kW was connected to the DG terminals. The power produced by the DG system was reduced from 125 kW to 90 kW, and a 25-kW three-phase linear local load was connected 1.25 s after the simulated range started.

The DG voltage amplitude was subsequently adjusted to exchange −10 kVAr with the grid. This was undertaken to obtain a minimal level of active (35 kW) and reactive (−10 kVAr) power through the grid, as seen in Fig. 11. Unlike what occurred in Section IV-C, the effects of islanding (at 3.0 s) followed by a reconnection [13] (at 5.0 s) were evident on the dc link voltage and power, or on the power flowing through the grid, with the most drastic case being the dc link power, which dropped to zero when the grid was reconnected.

VI. CONCLUSION

This paper presents an alternative solution to connecting a DG system to the grid, whereby the amplitude and displacement of the voltage synthesized by the DG is regulated with respect to the grid voltage and the control variable before and after the contingency is always the same by using Fuzzy Logic Controller. Additionally, a dc-dc step-up converter and a dc-ac VSI are used in a DG system as an interface with the power grid.

The simulation and experimental results demonstrate that the connection of DG sources can have adverse effects, depending on the connection procedures by Fuzzy Controller.

To improve the DG operation, the dc link voltage must be controlled, in this case by a dc-dc step-up converter. Fuzzy controller is associated with resonant regulators were used as a solution to produce

distortion-free DG voltage, even when the local load is nonlinear or when distortion occurs in the grid voltage. Although the PLL algorithm tracks as rapidly as possible, the frequency oscillations are slowly damped due to the limits of amplitude.

REFERENCES

[1] J. M. Carrasco *et al.*, "Power-electronic systems for the grid integration of renewable energy sources: A survey," *IEEE Trans. Ind. Electron.*, vol. 53, no. 4, pp. 1002–1016, Jun. 2006.

[2] S. B. Kjaer, J. K. Pedersen, and F. Blaabjerg, "A review of single-phase grid connected inverters for photovoltaic modules," *IEEE Trans. Ind. Appl.*, vol. 41, no. 5, pp. 1292–1306, Sep./Oct. 2005.

[3] M. Meinhardt and G. Cramer, "Past, present and future of grid connected photovoltaic- and hybrid power-systems," in *Proc. IEEE PES Summer Meet.*, 2000, vol. 2, pp. 1283–1288.

[4] M. Calais, J. Myrzik, T. Spooner, and V. G. Agelidis, "Inverter for singlephase grid connected photovoltaic systems—An overview," in *Proc. IEEE PESC*, 2002, vol. 2, pp. 1995–2000.

[5] J.M. A.Myrzik andM. Calais, "String and module integrated inverters for single-phase grid connected photovoltaic systems—A review," in *Proc. IEEE Bologna Power Tech Conf.*, 2003, vol. 2, pp. 1–8.

[6] F. Schimpf and L. Norum, "Grid connected converters for photovoltaic, state of the art, ideas for improvement of transformerless inverters," in *Proc. NORPIE*, Espoo, Finland, Jun. 2008, pp. 1–6.

[7] B. Liu, S. Duan, and T. Cai, "Photovoltaic DC-building-module-based BIPV system—Concept and design considerations," *IEEE Trans. Power Electron.*, vol. 26, no. 5, pp. 1418–1429, May 2011.

[8] L. M. Tolbert and F. Z. Peng, "Multilevel converters as a utility interface for renewable energy systems," in *Proc. IEEE Power Eng. Soc. Summer Meet.*, Seattle, WA, USA, Jul. 2000, pp. 1271–1274.

[9] H. Ertl, J. Kolar, and F. Zach, "A novel multicell DC–AC converter for applications in renewable energy systems," *IEEE Trans. Ind. Electron.*, vol. 49, no. 5, pp. 1048–1057, Oct. 2002.

[10] S. Daher, J. Schmid, and F. L. M. Antunes, "Multilevel inverter topologies for stand-alone PV systems," *IEEE Trans. Ind. Electron.*, vol. 55, no. 7, pp. 2703–2712, Jul. 2008.

[11] G. R. Walker and P. C. Sernia, "Cascaded DC–DC converter connection of photovoltaic modules," *IEEE Trans. Power Electron.*, vol. 19, no. 4, pp. 1130–1139, Jul. 2004.

[12] E. Roman, R. Alonso, P. Ibanez, S. Elorduizapatarietxe, and D. Goitia, "Intelligent PV module for grid-connected PV systems," *IEEE Trans. Ind. Electron.*, vol. 53, no. 4, pp. 1066–1073, Jun. 2006.

[13] F. Filho, Y. Cao, and L. M. Tolbert, "11-level cascaded H-bridge gridtied inverter interface with solar panels," in *Proc. IEEE APEC Expo.*, Feb. 2010, pp. 968–972.

[14] C. D. Townsend, T. J. Summers, and R. E. Betz, "Control and modulation scheme for a cascaded H bridge multi-level converter in large scale photovoltaic systems," in *Proc. IEEE ECCE*, Sep. 2012, pp. 3707 3714.

[15] B. Xiao, L. Hang, and L. M. Tolbert, "Control of three-phase cascaded voltage source inverter for grid-connected photovoltaic systems," in *Proc. IEEE APEC Expo.*, Mar. 2013, pp. 291–296.

[16] Y. Zhou, L. Liu, and H. Li, "A high-performance photovoltaic moduleintegrated converter (MIC) based on cascaded quasi-Z-source inverters (qZSI) using

eGaN FETs," *IEEE Trans. Power Electron.*, vol. 28, no. 6, pp. 2727–2738, Jun. 2013.

[17] J. Rodriguez, J. S. Lai, and F. Z. Peng, "Multilevel inverters: A survey of topologies, controls, and applications," *IEEE Trans. Ind. Electron.*, vol. 49, no. 4, pp. 724–738, Aug. 2002.

[18] Standard for Electric Installation and Use. [Online]. Available: https:// www.xcelenergy.com/

[19] A. Dell'Aquila, M. Liserre, V. Monopoli, and P. Rotondo, "Overview of PI-based solutions for the control of DC buses of a single-phase H-bridge multilevel active rectifier," *IEEE Trans. Ind. Appl.*, vol. 44, no. 3, pp. 857– 866, May/Jun. 2008.

[20] B. Xiao, K. Shen, J. Mei, F. Filho, and L.M. Tolbert, "Control of cascaded
H-bridge multilevel inverter with individual MPPT for grid-connected photovoltaic generators," in *Proc. IEEE ECCE*, Sep. 2012, pp. 3715– 3721.

BIOGRAPHIES:

R L S NAVEEN KUMAR Pursuing M.Tech in Electrical Power Systems in Teegala Krishna Reddy Engineering College Affiliated to JNTUH, Meerpet, Saroor Nagar, Ranga Reddy district, Telangana, India.

E-mail Id: nven.ravirala@gmail.com

C. SRINIVASULU currently working as a Associate Professor, Head of the Department in Teegala Krishna Reddy Engineering College Affiliated to JNTUH, Meerpet,Saroor Nagar, Ranga Reddy district, Telangana, India.

E-mail Id: eeedepttkrec@gmail.com